ELSEVIER

Modeling the state of marine ecosystems: A case study of the Okhotsk Sea

Costas A. Varotsos[a,*], Vladimir F. Krapivin[b]

[a] *Department of Environmental Physics and Meteorology, National and Kapodistrian University of Athens, Athens, Greece*
[b] *Kotelnikov Institute of Radioengineering and Electronics, Russian Academy of Sciences, Moscow, Russia*

A B S T R A C T

We provide an efficient tool for the processing of a large volume of data (big data) from a marine ecosystem and predicting its status, including its complex and nonlinear biological structure (biocomplexity) and its ability to remain alive or continue to exist (survivability). The Geoecological Information-Modeling System developed earlier by the authors of this paper is used for the first time as a basis for the development of the Sea Ecosystem Model that parameterizes the energy exchange between major trophic components of the sea with spatial resolution $1/6° \times 1/6°$ taking into account natural and anthropogenic factors. In particular, the dependence of energy exchange processes on environmental factors is modeled with a minimum level of uncertainty. The biological components are modeled using traditional trophic balance equations, whose coefficients are determined from observational data. The simulation results for the Okhotsk Sea show the critical ecosystem states that prevail when the biocomplexity and survivability of this ecosystem reach dangerous levels. The prediction of the ecosystem status is carried out to 2100 with an accuracy of better than 79.9%. For this purpose, the complex model proposed recently by the same authors, entitled "nature-society system model", was used. Among the main results that have emerged is that the biocomplexity and survivability characteristics of this marine ecosystem will be stable over the next 100 years, regardless of the expected climate change.

1. Introduction

The need to understand and predict changes in marine ecosystems is constantly growing due to the desire of a more encompassing approach to marine fisheries and environmental management that considers a wide range of the interacting groups within an ecosystem. Because organisms at higher trophic levels have a longer life span, with significant abundant variability and complex historical events with respect to microorganisms (further complicating their coupling to lower trophic levels and the natural system), the available biogeochemical and physical oceanographic models need to be expanded (Heath et al., 2004; Chattopadhyay et al., 2012).

Today, advanced analytical developments and statistical techniques are being used to improve the empirical robustness of marine ecosystem models by incorporating biochemical tracer data (e.g., compound-specific stable isotopes, fatty acids, and trace elements) and improve the accuracy of derived indices (Pethybridge et al., 2018).

Of particular interest is the Okhotsk Sea ecosystem (OSE) which is a unique natural system since it is relatively isolated from major human activities. However, over the last decades, global anthropogenic environmental effects have begun to impact this region with increasing intensity (Ohshima et al., 2009; Zhabin et al., 2010; Krapivin et al.,

2017b; Laurel and Copeman, 2018; Ide, 2018). Thus, the current situation of OSE pollution is progressively characterized by an increase in heavy metals flows, as well as various hazardous chemicals and organic compounds emitted by man-made activities of neighboring regions (Krapivin et al., 2016; Krapivin and Mkrtchyan, 2016). Significant potential sources of pollutants in the OSE include seven ports and the Amur River. It is expected that the level of OSE pollution will increase in the coming decades due to population growth in the Far-East regions of Russia and oil extraction on the shelf of the Kamchatka Peninsula. Therefore, the survivability of the system (i.e. its quantified ability to continue to function during and after a natural or man-made disturbance) is of crucial importance. It should be clarified at this point that survivability is a subset of resilience (i.e. the ability of a system to provide and maintain an acceptable level of service in the face of various faults and challenges to normal operation (Rohrer et al., 2014).

In addition, the geophysical and climatic conditions of Okhotsk Sea present many limiting factors for its ecosystem, including air temperatures, where in August it is about $14 °C$ and in February $-24 °C$. Consequently, the horizontal distribution of water temperature depends on the depth and vertical mixing that is the prerequisite for the productivity of the ecosystem. Average surface water temperature ranges from $-1.6 °C$ to $-1.8 °C$ in winter and from $6 °C$ to $14 °C$ in the

---

summer. The natural evolution of the OSE creates a unique geoecosystem with high productivity but low survivability. Therefore, the search for the criterion for assessing OSE survivability is critical and is suggested in this paper.

According to Krapivin et al. (2015), one of the indicators that determines the survivability level of the complex system is its biocomplexity. Michener et al. (2001) identified biocomplexity "… as property emerging from the interplay of behavioral, biological, chemical, physical, and social interactions that affect, sustain, or are modified by living organisms, including humans". This type of problem contains datasets that are too large or complex for traditional application software which are often termed as "big data" (Dedić and Stanier, 2017). It should be clarified that "cloud computing" refers to the platform for accessing large datasets. Hence, 'big data' is information and "big data cloud" is the means of getting information.

Meanwhile, OSE's ecological problems are the focus of the annual International Symposium on Okhotsk Sea and Polar Oceans, organized by Okhotsk Sea and Polar Oceans Research Association (Japan). This interest is explained by the concerns of Japan and Russia regarding the role of this region in climate change in relation to the further development of gas/oil resources in the Arctic region and in Sakhalin and Kamchatka, in particular (Ide, 2018). Many aspects of the problems that have arisen have been investigated by many authors. Aota et al. (1991, 1992, 2003) formulated the principles of the formation and structure of the controlled software of the automation system of data processing in the monitoring regime when the big data clouds are filtered and restored as the initial information for the Geoecological Information-Modeling System - GIMS (Varotsos and Krapivin, 2017). Legendre and Krapivin (1992) proposed a model of a phytoplankton community in the Arctic climate when ergocline ice/water plays an important role in the formation of biological productivity. Kelley and Krapivin (2004) introduced biocomplexity criteria for assessing OSE state based on big data processing, including satellite and in-situ monitoring data sources. Particular attention is paid to the estimation and mapping of sea-ice thickness (Tateyama et al., 2018; Kwok, 2010).

Takahashi et al. (1999), Ohshima et al. (2006) and Nihashi et al. (2009) noted that marine data has been growing exponentially over the last decade and should develop effective theoretical methodologies and practical applications of these data.

This paper develops a big data approach for the assessment of the marine ecosystem biocomplexity and survivability, which is based on existing monitoring data and guided by GIMS technology (Aota et al., 2003; Mkrtchyan and Krapivin, 2011; Kaevitser et al., 2013; Krapivin et al., 2015, 2016, 2017a,b). The model developed along these lines is applied to the OSE, which is an area of major economic interest, mainly for Japan and Russia.

2. Material and methods

2.1. Model description and its application to the Okhotsk Sea ecosystem

The big data description of the marine ecosystem is possible by using a complex model that allows the utilization of data of different quality and precision but also of different spatial and temporal diversity. Fig. 1 shows the structure of the Okhotsk Sea ecosystem model (OSEM) and Fig. 2 illustrates the OSE conceptual model of energy pathways and physical forcing mechanisms ("Atmosphere"). A conceptual diagram and the block contents of the OSEM are shown in Fig. 3 and defined in Table 1. Different components of the OSEM were considered in earlier published papers (Aota et al., 1991–2003; Kaevitser et al., 2013; Kelley and Krapivin, 2004; Krapivin, 2015; Krapivin and Soldatov, 2009; Krapivin et al., 2015, 2016). As it follows from Table 1, OSEM has the block structure, each of which describes a restricted set of processes which practically provides significant flexibility by allowing possible improvement of separate blocks.

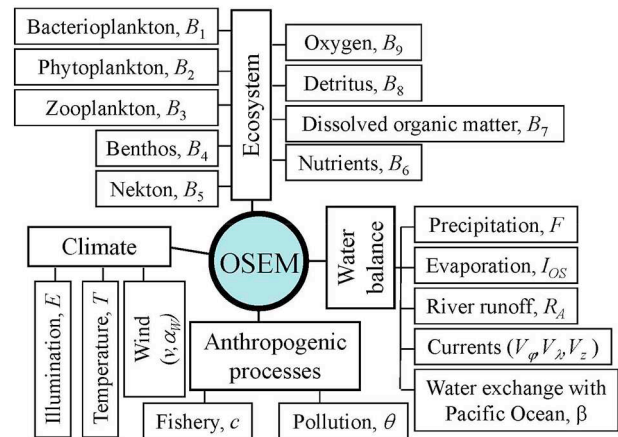The functioning of OSE is largely determined by severe climatic

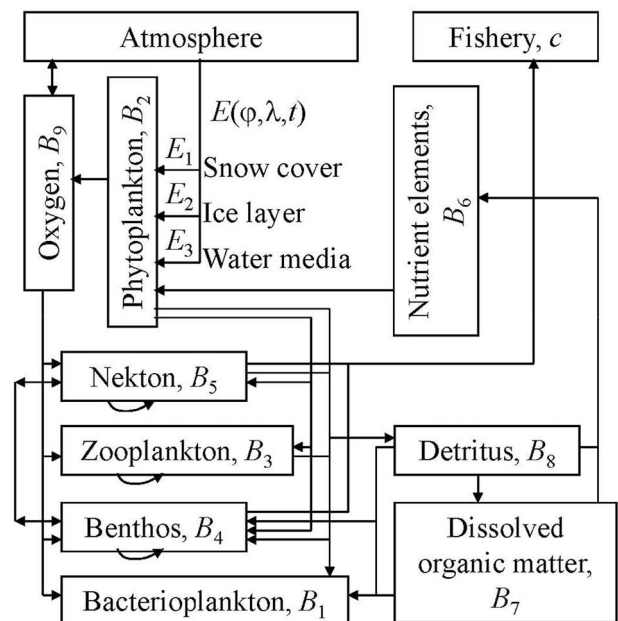**Fig. 1.** A block structure of OSEM and big data subjects.

Fig. 2. The conceptual structure of OSE energy fluxes.

conditions. The OSE is covered with 80–100 cm ice for 6–7 months a year. The extent of the ice cover is characterized by large inter-annual variations (Ohshima and Martin, 2004; Ohshima et al., 2006; Matoba et al., 2011). In this context, the structure of the OSE surface environment exhibits a high degree of variability that evolves seasonally. The thermal regime that determines this structure is formed by large-scale cyclonic and anti-cyclonic processes whose activity changes during winter and summer according to global climate trends in the OSE region and in the neighboring zones (Ohshima et al., 2009; Varotsos and Efstathiou, 2013, 2019). OSEM has two mechanisms for modeling the ice fields:

- viewing satellite images at discrete time intervals and interpolation; and
- using models such as the Discrete-Element Model (Herman, 2016).

OSEM allows the optimization of the monitoring regime and the supply of its input data to the operational regime of the geo-ecosystem of the Okhotsk Sea. A basic structure of such a step-type tracking procedure is given in Fig. 4 which implements the GIMS technology (Mkrtchyan and Krapivin, 2011). This technology illustrates the support for the adaptive regime for the simulation experiment when OSEM
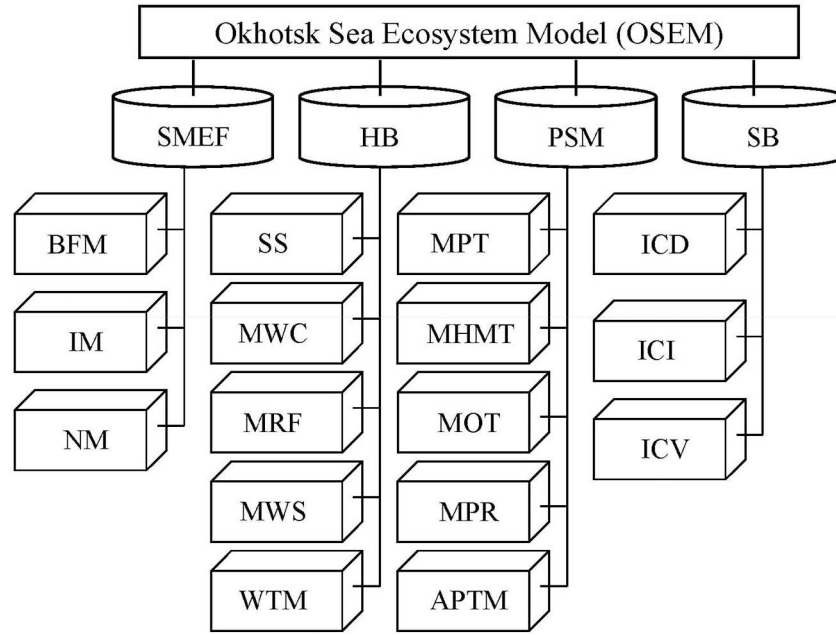
Fig. 3. Block diagram of the OSEM. Description of the blocks are given in Table 1.

Table 1
Description of the OSEM blocks.

Block	The block description
SMEF	The set of models for energy flows in the trophic chains of the Okhotsk Sea ecosystem.
HB	Hydrological block describing the water circulation in Okhotsk Sea and the movement of ecological elements.
PSM	Pollution simulation model of the Okhotsk Sea basin, including the set of anthropogenic scenarios.
SB	Service block to control the simulation experiment.
APTM	Air pollution transport model.
BFM	The biota functioning model under the conditions of energy exchange in the trophic chains of the Okhotsk Sea ecosystem.
SS	Simulator of scenarios describing the ice fields, the synoptic situations and changes in the hydrological regimes.
MWC	Model of the water cycle in the Okhotsk Sea basin.
MHMT	Model of heavy metals transport through the food chains.
IM	The illumination model.
NM	The Nutrients Model.
MPT	Model for pollution transport through water-exchange between Okhotsk Sea and the Pacific Ocean.
MOT	Model for the process of oil hydrocarbon transport to the food chains.
MPR	Model for the process of radionuclide transport to the food chains.
MRF	Model of the river flow to the Okhotsk Sea.
MWS	Model of the water salinity dynamics.
WTM	The water temperature model.
ICI	Interface for control of identifiers.
ICD	Interface for control of the database.
ICV	Interface for control of the visualization.

is regularly updated according to the precision of the modeling results.

The OSE domain Ω is modeled as a 3-dimensional grid with horizontal grid $\{\Omega_{ij}\}$ resolution $\Delta\varphi \times \Delta\lambda$ by the latitude φ and longitude λ and vertical resolution Δz defined by depth z. Big data clouds are formed taking into account this grid cell structure $\Omega_{ij} = \{(\varphi,\lambda): \varphi \in [\varphi_i, \varphi_i + \Delta\varphi], \lambda \in [\lambda_j, \lambda_j + \Delta\lambda]\}$. Note that OSE trophic balance equations are solved according to this grid cell structure.

The dynamic equation for the biomass of the i-th living component is written in the following form:

$$\frac{\partial B_i}{\partial t} + V_\varphi \cdot \frac{\partial B_i}{\partial \varphi} + V_\lambda \cdot \frac{\partial B_i}{\partial \lambda} + V_z \cdot \frac{\partial B_i}{\partial z} = R_i - Y_i - M_i - \sum_{s \in \Gamma_i} C_{is} R_s + k_\varphi$$
$$\cdot \frac{\partial^2 B_i}{\partial \varphi^2} + k_\lambda \cdot \frac{\partial^2 B_i}{\partial \lambda^2} + k_z \cdot \frac{\partial^2 B_i}{\partial z^2}, \ (i = 1 - 5);$$

(1)

$$\text{where:} C_{is} = k_{is} \cdot \frac{\overline{B_i}}{\sum_{m \in S_j} k_{sm} \cdot \overline{B_m}},$$

(2a)

$$\overline{B_i} = max\{0, B_i - B_{i,min}\},$$

(2b)

$$Y_i = \tau_i \cdot B_i^{\omega_i}, \quad M_i = (\mu_i + \mu_i^* \cdot B_i) \cdot B_i$$

(2c)

$$R_i = \begin{cases} \eta_i \left(1 - \exp\left[-\nu \sum_{s \in S_i} \overline{B_s}\right]\right), i = 1, 3, 4, 5; \\ min \ \{\rho B_2, aB_2 [1 - \exp(-qB_6)] E \exp[b(1 - E/E_{max})]\}, \ i = 2; \end{cases}$$

(3)

where R_i is the production, Y_i is the energy exchange losses, M_i is the mortality, $k(k_\varphi, k_\lambda, k_z)$ is the components of the turbulent diffusion coefficient, Γ_i is the set of the trophic subordination of the i-th component, $B_{i,min}$ is the minimum biomass of the i-th component consumed by other trophic levels; η_i ($i = 1$: 500; $i = 3$: 200; $i = 4$: 900; $i = 5$: 800 mg/m^3/day) is the maximal ratio of i-th component under the food excess, ν (0.26×10^{-3} m^3/mg) is the starvation level coefficient, q (0.013 m^3/mg-atom) is the effective index of nutrient salts, ρ (0.05 day^{-1}) and a (0.07 day^{-1}) are the phytoplankton productivity coefficients under the absence and presence of limiting factors, respectively; b (0.2) is the coefficient of illumination effect. τ_i (0.01–0.05 day^{-1}) and ω_i (0.69–0.95) are the coefficients characterizing the dependence of the respiratory losses on temperature and oxygen saturation, respectively; k_{sm} (0.01–0.4) is the trophic-load coefficient between levels s and m.

The dependencies of living processes on environmental parameters are described by the following equations, taking into account Kleiber's and Arrhenius's laws (Kleiber, 1932; Knies and Kingsolver, 2010; Varotsos and Zellner, 2010):
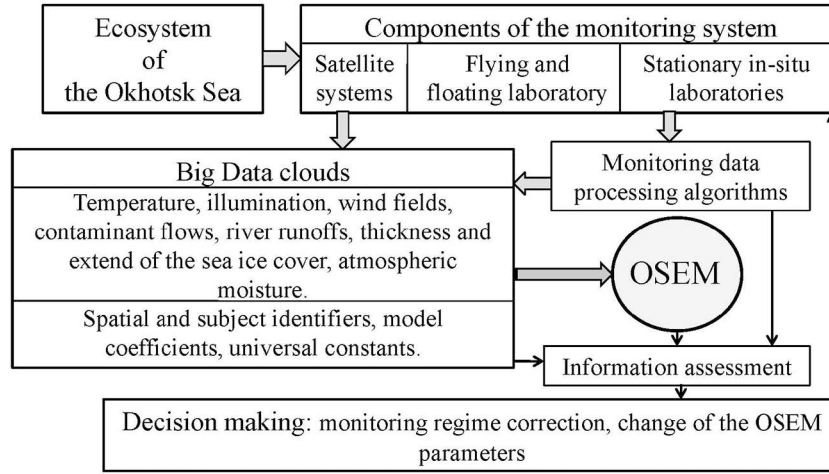
Fig. 4. A basic scheme for using big data tools to assess the OSE survivability.

$$\tau_i(B_9, T) = \begin{cases} \xi_i(T) & if \ B_9 > B_{9,min}; \\ \xi_i(T)B_9/B_{9,min} & if \ 0 \le B_9 \le B_{9,min} \end{cases} \xi_i(T)$$

$$= \begin{cases} \chi_i & if \ T \in [T_1^i, T_2^i]; \\ \chi_i [d_i \exp(-c_i |T|)]^{S_i} & if \ T \notin [T_1^i, T_2^i] \end{cases} \quad (4)$$

$$\mu_i^* = \mu_0^i \cdot \mu_i(B_9, T, \theta); \quad (5)$$

$$\mu_i = p_1^i \exp\{\varepsilon_1^i [1 - B_9/B_{9,min}]\}(1$$
$$+ p_0^i \Delta\theta) \begin{cases} 1, & if \ T \in [T_1^i, T_2^i]; \\ \exp\{p_2^i(T - T_1^i)(T - T_2^i)\} & if \ T \notin [T_1^i, T_2^i]; \end{cases} \quad (6)$$

where T_1^i ($-0.8\,°C$) and T_2^i ($12\,°C$) are minimal and maximal temperatures for the temperature adaptation zone of i-th living element, respectively; $S_i = 0.5(T_1^i + T_2^i)/m_i$; m_i (10), d_i (0.9) and c_i (0.038 $°C^{-1}$) are constant; p_1^i (0.1 day^{-1}) is the pre-exponential mortality factor; ε_1^i (0.042) is the oxygen-limiting coefficient; p_0^i (0.002 1/%) is the pollution-mortality coefficient; p_2^i (-3.97) is the temperature-efficiency coefficient; χ_i (0.01–0.05 day^{-1}) is the respiration rate for i-the component. μ_0^i (0.01) is the mortality-factor due to overpopulation;

Trophic balance equations for the B_i ($i = 6$–9) have the following forms:

$$\frac{\partial B_6}{\partial t} + V_\varphi \cdot \frac{\partial B_6}{\partial \varphi} + V_\lambda \cdot \frac{\partial B_6}{\partial \lambda} + V_z \cdot \frac{\partial B_6}{\partial z} = \mu_d \cdot B_8 - \mu_p \cdot R_2 + \rho_r \cdot B_7 + k_\varphi$$
$$\cdot \frac{\partial^2 B_6}{\partial \varphi^2} + k_\lambda \cdot \frac{\partial^2 B_6}{\partial \lambda^2} + k_z \cdot \frac{\partial^2 B_6}{\partial z^2}; \quad (7)$$

$$\frac{\partial B_7}{\partial t} + V_\varphi \cdot \frac{\partial B_7}{\partial \varphi} + V_\lambda \cdot \frac{\partial B_7}{\partial \lambda} + V_z \cdot \frac{\partial B_7}{\partial z} = \sum_{i=1}^{5} (1 - \xi_{Oi})Y_i - c_r \cdot R_1 + c_\varphi \cdot R_2 + k_\varphi$$
$$\cdot \frac{\partial^2 B_7}{\partial \varphi^2} + k_\lambda \cdot \frac{\partial^2 B_7}{\partial \lambda^2} + k_z \cdot \frac{\partial^2 B_7}{\partial z^2}; \quad (8)$$

$$\frac{\partial B_8}{\partial t} + V_\varphi \cdot \frac{\partial B_8}{\partial \varphi} + V_\lambda \cdot \frac{\partial B_8}{\partial \lambda} + V_z \cdot \frac{\partial B_8}{\partial z} = \sum_{i=1}^{5} M_i - \mu_d \cdot B_8 - c_d \cdot R_1 + k_\varphi$$
$$\cdot \frac{\partial^2 B_8}{\partial \varphi^2} + k_\lambda \cdot \frac{\partial^2 B_8}{\partial \lambda^2} + k_z \cdot \frac{\partial^2 B_8}{\partial z^2}; \quad (9)$$

$$\frac{\partial B_9}{\partial t} + V_\varphi \cdot \frac{\partial B_9}{\partial \varphi} + V_\lambda \cdot \frac{\partial B_9}{\partial \lambda} + V_z \cdot \frac{\partial B_9}{\partial z} = -\sum_{i=1}^{5} \xi_{Oi} Y_i - \mu_O \cdot \mu_d \cdot B_8 - c_O \cdot R_2 + k_\varphi$$
$$\cdot \frac{\partial^2 B_9}{\partial \varphi^2} + k_\lambda \cdot \frac{\partial^2 B_9}{\partial \lambda^2} + k_z \cdot \frac{\partial^2 B_9}{\partial z^2}; \quad (10)$$

where μ_d (0.1 day^{-1}) is the indicator of detritus decomposition rate, μ_p (0.1) is the indicator of the nutrient uptake rate in the phytoplankton, ρ_r

(0.05 day^{-1}) is the indicator of nutrient increment rate from DOM, c_r (0.56) is the relation coefficient of bacterioplankton/DOM, c_d (0.25) is the detritus-uptake bacterial factor, ξ_{Oi} (0.8) is the oxygen-uptake coefficient, μ_O (0.013) is the oxygen-uptake rate in detritus decomposition process, c_O (0.012) is the oxygen-increment rate in the photosynthesis process; c_Φ (0.04) is the supply-indicator of the rate of replenishing the DOM due to the photosynthesis.

2.2. Biocomplexity and survivability indicators

Transition processes in the OSE may be accompanied by a biocomplexity change indicator, which can be a precursor to the critical states that may arise from climate change and pollution (e.g. Xue et al., 2014). Biocomplexity derives from biological, physical, chemical, and social factors occurring in the OSE region (Krapivin, 2015; Krapivin and Soldatov, 2009; Krapivin and Varotsos, 2016; Krapivin et al., 2016). The impact of these factors on the OSE can change the biodiversity and distort the energetic interactions between its living elements. As a result, OSE can change its behavior and structure and change the level of survivability for all sub-systems. The existence or absence of trophic interactions between OSE elements is the defined function C_{is} in (2). Subsequently, the biocomplexity indicator is as follows:

$$I(\varphi, \lambda, z, t) = \sum_{i=1}^{8} \sum_{s=1}^{5} x_{is} C_{is} \quad (11)$$

where

$$x_{is} = \begin{cases} 1, & if \ B_i \ge B_{i,min} \\ 0, & if \ B_i < B_{i,min} \end{cases} \quad (12)$$

Relationship (11) reflects the OSE state depending on the season. The maximal level of $I(\varphi, \lambda, z, t)$ is achieved during the spring-summer period at the expense of productivity growth of all living components with a sharp change of production/biomass P/B coefficient from 0.2 to 0.9 in many parts of the Okhotsk Sea. Estimates of the production and biomass ratio are one measure for the assessment of the ecosystem health (Ikeda et al., 2002). The OSE production has significant variations during the year. For example, bacterial production is observed in the large range from 0.08 $mgC/dat/m^3$ to 55 $mgC/dat/m^3$ (Zakharkov et al., 2017). The limiting factors reduce biocomplexity in the zones of oxygen deficit, low temperatures and pollution. This effect is described by the functions Y_i and M_i in Eqs. (1)−(10) whose coefficients are a function of environmental parameters.

The biocomplexity of the limited aquatory Ω_{ij} is calculated using the following model:
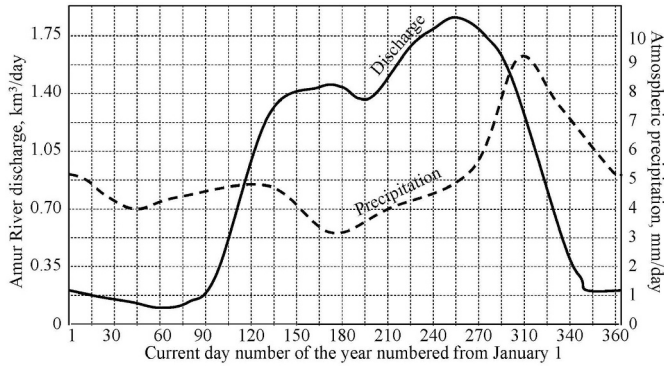
Fig. 5. The annual distribution of the Amur River discharge and precipitation in the Okhotsk Sea region.

$$I_{\Omega_{ij}}(t) = \frac{1}{\sigma_{ij}} \cdot \iiint\limits_{(\varphi,\lambda,z)\in\Omega_{ij}} I(\varphi,\lambda,z,t)\, d\varphi\, d\lambda\, dz \tag{13}$$

where σ_{ij} is the grid cell Ω_{ij} area.

Finally, OSE survivability is estimated by the following equation:

$$J(t) = \frac{\iiint\limits_{(\varphi,\lambda,z)\in\Omega} I(\varphi,\lambda,z,t)\, d\varphi\, d\lambda\, dz}{\iiint\limits_{(\varphi,\lambda,z)\in\Omega} I(\varphi,\lambda,z,t_0)\, d\varphi\, d\lambda\, dz} \tag{14}$$

Indicator $J(t)$ reflects the evolution of the sea ecosystem biocomplexity relative to its initial state, depending on the environmental factors (see Eq. (2)).

In the following, the simulations results obtained from the implementation of the above described model in the OSE will be presented as a demonstration of its capabilities. The Amur River runoff R_A and precipitation F are described with the seasonally changing rates shown in Fig. 5.

3. Simulation results

3.1. Characteristics of the marine system

A reliable assessment of OSE evolution requires the determination of OSEM coefficients and the spatial interconnection of big data clouds. The spatial horizontal grid scale is $\Delta\varphi = \Delta\lambda = 1/6°$. Important characteristics of the Okhotsk Sea are given in Table 2.

The OSEM model simulations were initialized on January 1, 2015 as defined in Table 3 where all B_i ($i \neq 5$) components are uniformly distributed with a depth of 0–200 m. Additional fluxes of nutrients into river runoff and water exchange with the Pacific Ocean are taken into account through corresponding changes in boundary grid cells. The simulation time-step is one day.

3.2. The biocomplexity of a marine ecosystem

Many simulation experiments have shown that OSE's state is dependent on initial conditions only during the first 15–30 days, thus forming the traditional vertical structure of the ecosystem. Indeed, OSEM forgets the initial conditions and changes, depending on the modeled environment, including variations of temperature, river runoff and pollution.

Climate change at Arctic and Sub-Arctic latitudes will affect the metabolic demands of OSE living elements that lead to the transformation of nutritional relationships between them (Laurel and Copeman, 2018). Temperature-dependent effects are independent determinants of OSE evolution and are the main cause of predicting climate change impacts of OSE.

Fig. 6 shows results of simulations in which the sea surface

Table 2
Basic characteristics of OSE.

Parameter	Parameter value
Area (10^3 km^2):	
without Kuril islands	1582.8
without all islands	1579.9
without gulfs	1385.1
Coastline (km)	10,444
Sea volume (10^3 km^3)	1208.3–1227.7
Specific depths (m):	
maximal	3379–3953
average	765–777
Average annual atmospheric temperature (°C):	
on the north	−7
on the south	+5.5
Annual river runoff (km^3/year)	585
November–April (%)	10–15
May–October (%)	85–90
Continental runoff (mm/year)	370
Precipitation on the sea surface (mm/year)	500
Evaporation from the sea surface (mm/year)	300
Annual amplitude of average monthly temperature of surface water layer (°C)	10–15
Surface water temperature (°C):	
winter	- 1.8 to +2
summer	+10 to +18
Water salinity (‰)	29–34

Table 3
Initial data for the OSEM-experiment started on 1 January 2015.

| Component	The Okhotsk Sea basin				
	Western	Eastern	Northern	Southern	Central
Bacterioplankton, mg/m^2	63	82	45	120	51
Chrolophyll-a, mg/m^3	2.1	1.9	1.4	2.5	1.3
Zooplankton, g/m^2	61	92	52	110	87
Bentos, mg/m^3	7.1	7.1	7.1	7.1	7.1
Nekton, mg/m^3	20	20	15	25	10
Nutrient salts, mg/m^3	45	45	45	45	45
DOM, g/m^3	1.5	0.9	0.8	1.3	1.9
Detritus, g/m^3	0.8	0.8	0.8	0.8	0.8
Oxygen	9.2	9.2	9.2	9.2	9.2
Water temperature, °C	−1.8	−0.5	−1.2	−0.2	−0.9
Water salinity, ‰	30	30	30	30	30
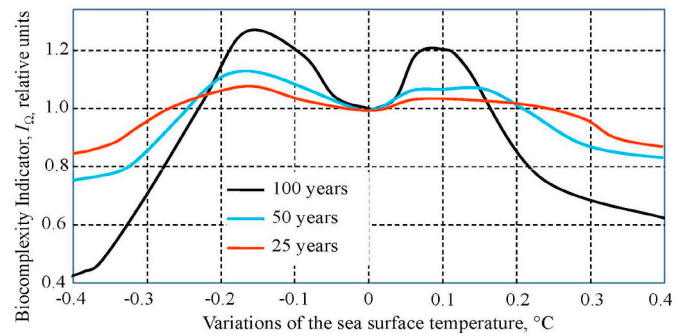
Fig. 6. The OSE biocomplexity depends on the sea surface temperature change over 25, 50 and 100 years. The results are given relative to the biocomplexity indicator value in the absence of temperature variations.

temperature can vary over a limited time. As can be seen from these results, the OSE biocomplexity changes by ± 20% when the sea surface water temperature changes by ± 0.4 °C during no more 50 years. Long-term temperature changes above ± 0.2 °C lead to a rapid reduction of OSE biocomplexity. It states that the OSE trophic pyramid is dependent on thermal conditions. Certainly, there are more temperature-tolerant species, while the distinct ontogenetic thermal response is determined
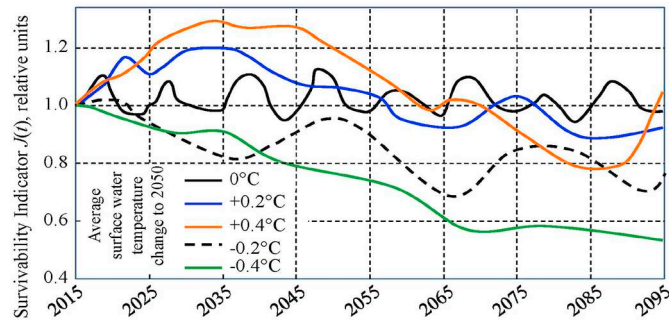
Fig. 7. The OSE survivability depending on the average water temperature change.

by wider temperature variations. The results of Fig. 6 show only a specific example when the biocomplexity indicator is calculated as an integral feature of OSE.

3.3. The survivability assessment of a marine ecosystem

Fig. 7 examines scenarios of linear change in surface water temperature by 2050 and presents the OSE survivability assessment. It seems that the OSE survivability index is stable and changes when the temperature variations do not exceed ± 0.2 °C and + 0.4 °C. In these cases, the survivability indicator shows the existence of stable variations over several decades. However, Fig. 6 shows that the decrease of temperature even by 0.2 °C leads to the slow decrease of ecosystem survivability. It shows that the temperature regime of the Okhotsk Sea ecosystem is a significant factor of its evolution. Table 4 shows the OSE survivability indicator for different depths and seasons. It is obvious that the upper layer of 150 m is the most stable and productive. Near the sea bottom, the ecosystem is more vulnerable. A general representation of the OSE's biocomplexity distribution is given in Fig. 7. These results are accompanied by typical trends in the specific OSE characteristics. For example, the relationship of photosynthesis/respiration varies widely (average 4.7) and primary production variations is 78 gC/m^2/yr (average 352 gC/m^2/yr). The P/B ratio changes from 0.2 to 0.9 during the spring-summer season reaching 0.7–0.9 in the southern region, the Kuril Islands and near the western Kamchatka (Zakharkov et al., 2017). The results of Fig. 8 illustrate all these variations as an indispensable index of the OSE state. These results show that the OSE biocomplexity and survivability characteristics will be stable over the next 100 years, regardless of the expected climate change. At this point it is worth mentioning the periodicities that appear in the graphs of Fig. 7 ranging from about 11 to about 100 years, referring to climatic data (e.g., Efstathiou and Varotsos, 2010, 2012, 2013; Varotsos, 1987, 2013; Varotsos and Cartalis, 1991). Of course, in addition to normal fluctuations, the climate system also exhibits irregular fluctuations, especially when it is in an unstable equilibrium (Varotsos, 2002, 2003, 2004; Varotsos et al., 2014, 2019).

Sensitivity analysis of OSE's responses to environmental changes includes the potential impacts of factors whose intensity is currently insignificant. The most dangerous effects in the future are those that can affect the OSE oxygen cycle leading to hypoxic conditions. This

Table 4
The survivability indicator as a function of the water depth. The data are normalized relative to their maximum.

Season	Layer, m				
	0–30	30–150	150–750	750–1500	> 1500
Spring-summer	0.98	0.99	0.72	0.47	0.23
Winter	0.32	0.61	0.76	0.54	0.28

phenomenon is due to the pollution of the water environment, including inputs of nitrates, nitrites, phosphates and other nutrient salts whose sources are terrestrial, mainly delivered via Amur River runoff (Zhabin et al., 2010). The oxygen deficiency in water can be caused by the inflow of oil products into the OSE through river runoffs and navigation processes. The eastern sections of the Sea of Okhotsk are highly productive with few local sources of pollution, contributing to persistently high levels of oxygen saturation. The OSEM allows for the hypothetical consideration of scenarios with the assessment of OSE reactions to water pollution from river runoff of nutrients, heavy metals, radionuclear pollutants and oil hydrocarbons (Krapivin et al., 1998, 2015; Krapivin and Ba Lan, 1995). Preliminary simulations show that a possible increase by no > 5% over current levels of oil hydrocarbon pollution does not lead to an oxygen deficit, but reveals a trend of decreasing oxygen levels and formation of oxygen minimum zones.

Observed changes in OSE are characterized by increased water temperature, decreased dissolved oxygen and increased variations in the extent of sea-ice (Kwok, 2010; Matoba et al., 2011). OSEM calculates the sea-ice extent Σ_{ij} in each grid cell Ω_{ij} using the following equation: $\Sigma_{ij} = \omega_{ij}\sigma_{ij}$, where ω_{ij} is the ice-production coefficient (Nihashi et al., 2009):

$$\omega_{ij}(\varphi,\lambda) = \exp\{\alpha_{ice}\cdot[T(\varphi,\lambda) - T_{min}(\varphi,\lambda)]/[T_{max}(\varphi,\lambda) - T_{min}(\varphi,\lambda)]\};$$
$$(\varphi,\lambda) \in \Omega_{ij} \tag{15}$$

where T_{max} and T_{min} are the maximal and minimal surface water temperatures at the grid cell $1/6° \times 1/6°$ during the ice-formation period, α_{ice} (1.92) is the ice-formation coefficient.

OSEM validation was based on a comparison of monitoring data and the modeling of relative sea ice cover and net primary production. The OSEM validation characteristics are listed in Table 5.

It is known that the extent of the sea ice in the Okhotsk Sea over the last 30 years has decreased by about 10% and the ice cover formation process is a function of a global temperature increase (see Fig. 9). Therefore, if the average air temperature of the OSE region has increased by about 2.0 ± 1.4 °C over the past 50 years, the global temperature increase has been characterized by 0.74 ± 0.6 °C over the past 100 years. Consequently, comparative data in Table 5 should be considered as a qualitative comparison.

The biological and hydrological processes in the Sea of Okhotsk are functions of the sea-ice extent and its duration during the year. In this regard, OSEM takes into account the results obtained by Legendre and Krapivin (1992) and Edvardsen et al. (2002). Sea-ice cover mainly affects illumination attenuation (Fig. 2, Block IM). It is assumed that the role of chrolophyll-a in snow and ice is not significant and does not affect the vertical distribution of algal biomass. According to Krapivin et al. (2017b), OSEM allows the formation of sea-ice fields in their dynamics (Fig. 10).

The main indicator of the effects of particular hazardous anthropogenic influence is the variation in nutrient concentration which determines the ecosystem's capability for stable evolution. Table 6 characterizes ecosystem response to variation of initial concentration. In this case, the initial phytoplankton biomass was $B_2(t_0,\varphi,\lambda,z) = 1.8$ mg/m^3. We see that the ecosystem, under other standard environmental parameters, overcomes the nutrient deficit and proceeds to become stable over time. Low initial nutrient conditions are overcome within roughly 50 days. This result demonstrates one use of the OSEM. Mainly, OSEM allows the consideration of spatial distributions of external impacts and modeling results.

4. Discussion

Although, there are numerous publications on changes in the marine ecosystem due to global climate change and the increasing anthropogenic impacts, this issue is still purely understood. This is because there is a need for combined analysis of big data clouds that are
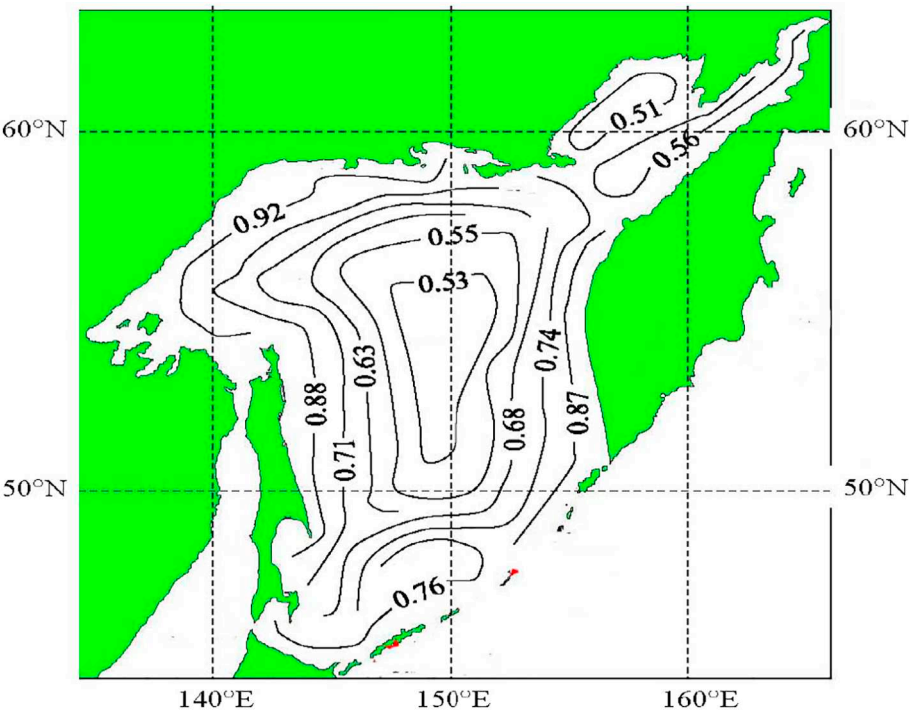
Fig. 8. The spatial distribution of the OSE biocomplexity indicator $I_\Omega/I_{\Omega,max}$ for the spring-summer season.

characterized by heterogeneity, nonstructure, instability and diversity (Lovejoy and Varotsos, 2016; Varotsos et al., 2019). The proposed model in this paper allows the ability to organize the processing of these data for a complex geo-ecological system and to predict its evolution. The results obtained from this model demonstrate these capabilities and show the effectiveness of this model to address the different scenarios of the marine ecosystem's interaction with its surrounding environment.

When implementing this model in the Sea of Okhotsk, many simple-model processes are described to reduce unknown parameters which help to avoid many uncertainties and possible errors. Another important feature of this approach is the use of a simple climate model by Mintzer-Sergin (Krapivin et al., 2015) for calculating the daily temperature according to trends in greenhouse gases emissions. Simulations include OSEM blocks as currents, water exchange with the Pacific Ocean and Amur River runoff (Belkin and Cornillon, 2004; Zhabin et al., 2010). Surface circulation and tidal currents of the Okhotsk Sea are given as a distribution of the parameters (ν, α_W) per grid cell Ω_{ij} in the summer and winter (Takahashi et al., 1999). Water exchange between the Sea of Okhotsk and the Pacific Ocean changes the water salinity, temperature, and oxygen in grid cells located near Kuril Islands. Although OSEM has components that require high accuracy, it allows assessing and predicting OSE parameters under various preliminary scenarios of global climate change and the qualitative change of anthropogenic processes in the Okhotsk Sea region. Figs. 6–10 clearly show the existence of dangerous environmental changes when the OSE can transform its state.

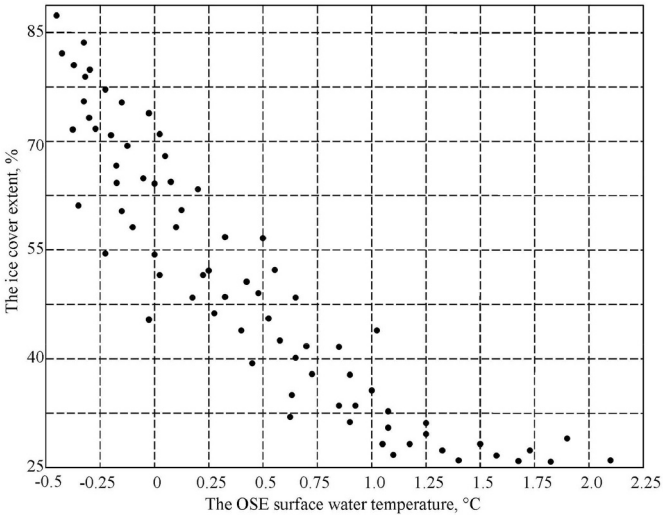Under the acceptable constraints, a relatively reliable spatial

Fig. 9. Observational data for the comparative analysis of the correlations between the sea-ice cover extent and the surface layer temperature of the Okhotsk Sea (Kwok, 2010; Matoba et al., 2011; Ohshima et al., 2006).

structure of OSE develops with observed distributions of its components as they evolve. A long-term downward trend in sea-ice by $0.037 \times 10^6 \, km^2$ (2.25%) per decade is observed as followed by Fig. 8. The increase or decrease in water temperature of more than $\pm \, 0.25 \, °C$,

Table 5
The OSEM validation data.

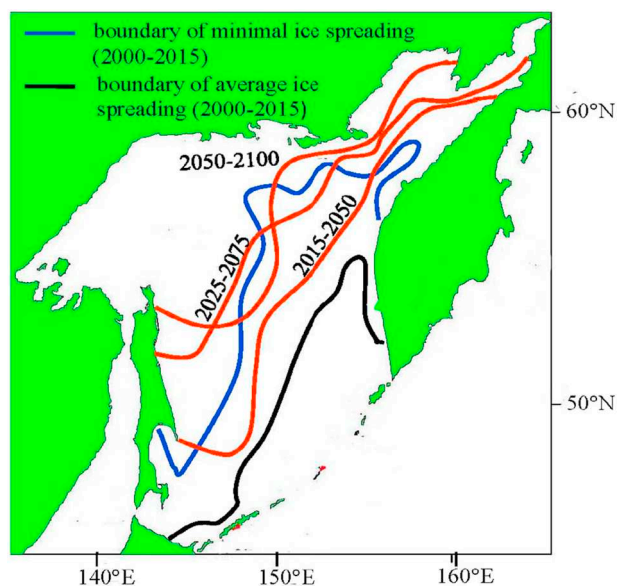| Season	Sea ice extent			Average net primary production, $gCm^{-2} \, yr^{-1}$		
	Monitoring data	The OSEM result	The OSEM precision, %	Observational data	The OSEM result	The OSEM precision, %
2015	39.9%	44.2%	89.1%	449	539	79.9%
2016	69.4%	63.3%	91.2%	391	464	81.4%
2017	64.6%	72.6%	87.6%	436	509	83.2%

Fig. 10. The results of the OSEM calculations for sea-ice extent with a forecast of up to 2100. The red lines correspond to the average ice spread over a limited period of time. (For interpretation of the references to colour in this figure legend, the reader is referred to the web version of this article.)

Table 6
The OSE reaction to alternate initial nutrient concentrations (B_6).

Depth, z (m)	Phytoplankton biomass (g/m³)							
	$B_6(t_0,\varphi,\lambda,z) = 0.045\,mg/m^3$.				$B_6(t_0,\varphi,\lambda,z) = 3.2\,mg/m^3$.			
	$t - t_0$ (days)							
	10	30	50	70	10	30	50	70
0	0.97	4.78	9.32	10.72	6.33	11.35	10.87	12.83
10	1.83	5.03	11.37	12.34	5.45	12.34	16.81	15.98
20	2.44	9.56	19.18	21.56	7.12	19.32	22.11	21.18
30	1.21	6.12	18.43	18.43	7.46	14.59	14.95	14.87
40	0.57	2.97	8.96	9.26	5.58	10.15	9.76	10.15
50	0.18	1.54	8.34	8.75	4.27	7.76	8.45	8.43
70	0.09	0.89	5.27	5.36	1.75	4.84	5.12	5.17
100	0	0.38	2,12	2.14	1.18	1.98	2.23	1.97
150	0	0.12	0.92	0.95	0.84	1.17	1.39	1.42
200	0	0.09	0.14	0.16	0.21	0.34	0.26	0.27

as shown in Figs. 4 and 5, has a negative impact on OSE evolution. Relatively good results are obtained for the spatial distribution of water salinity: it is constantly decreasing from 27.5 to 29.9‰ to western grid cells at 30.8–31.7‰ in eastern grid cells under its reduction to 25.2‰ in separate northwestern grid cells and its growth up to 33.6‰ near Sakhalin Island. Existing pollution levels by oil hydrocarbons under a possible increase by no more 5% do not lead to oxygen deficiency. However, when the concentration of oil hydrocarbons reaches 3 ppm at each grid cell, the saturation of oxygen in water in separate regions may fall to a fatal level of 0.2 ml/l.

OSEM allows for the spatial distribution of biomass of living elements and the evaluation of their productivity depending on the change in environmental parameters. For example, the spatial distribution of phytoplankton biomass is characterized by significant fluctuations ranging from 900 mg/m³ in coastal grid cells to 20,000 mg/m³ near Shantar Islands. This variation is reduced by 56% over the next 50 years with global warming by 0.5 °C. In this case, the total production of the OSE amounts to the maximum level at 2075 and then begins to decrease. Negative effects result from the increase in surface water temperature by 0.4 °C and higher (see Fig. 6). Accordingly, annual changes

in zooplankton biomass from 1500 mg/m³ in 2015 (Edwards and Brindley, 1999; Volkov, 2018) are reduced by 9.1% and 11.2% in 2050 and 2100, respectively. The spatial distribution of zooplankton biomass in the top layer 0–25 m is smoother.

Thus, OSEM is a prospective tool for the deliberate processing of big data characterizing ecological processes at OSE with the prognosis of its biocomplexity and survivability. The mismatches between the real and acceptable values of the model parameters as shown in Table 5 can be the source of errors in the prognostic results. Improvement of different model blocks by parameterizing mainly hydrological and anthropogenic processes will make OSEM's results more reliable. However, there is a risk of introducing additional uncertainties into modeling results. It is evident that OSEM needs improvement for the most reliable assessment of the production of fish and other commercial species. For this purpose, it is necessary to include additional blocks in OSEM (Shirasawa et al., 2017).

5. Conclusion and outlook

As has been demonstrated from the above, a big data model may be applied for assessing biocomplexity and survivability of a marine ecosystem. This approach is based on existing monitoring data and geoecological information technology.

This model was applied to the Okhotsk sea ecosystem and the conclusions drawn are as follows:

- the state of this ecosystem depends on the initial conditions only during the first 15–30 days and becomes independent of initial conditions in later years.
- the survivability of this ecosystem changes by ± 20% when the temperature of the sea surface water changes by ± 0.4 °C in < 50 years. Its survivability index is stable and changes when the temperature variations do not exceed − 0.4 °C. Its variability with depth indicates that the top 150 m are the most stable and productive, while the ecosystem is more vulnerable to the bottom of the sea.
- the biocomplexity of this ecosystem decreases rapidly when the long-term temperature changes more than ± 0.2 °C.
- the biocomplexity and survivability characteristics of this ecosystem will be stable over the next 100 years, regardless of the expected climate change, if the increase in the global average temperature does not exceed 1.5 °C and the regional temperature in the Okhotsk Sea zone does not increase by > 0.4 °C.
- the observed variation in the spatial distribution of phytoplankton biomass between 900 and 20,000 mg/m³ will be reduced by 56% over the next 50 years due to global warming by 0.5 °C.
- under expected levels of climate change, the total production of the Okhotsk sea ecosystem will reach its peak in 2075 and then begin to decline.
- the annual changes in zooplankton biomass from 1500 mg/m³ in 2015 will decrease by 9.1% and 11.2% in 2050 and 2100, respectively.

It is obvious that the developed model needs improvement for the most reliable assessment of the production of fish and other commodities. For this purpose, it is necessary to add additional blocks to this model. Moreover, it is necessary to assess the OSE survivability according to the levels of pollution and the more detailed estimates of OSE changes due to global warming. We intend to use OSEM to study in detail the OSE survivability according to different hypothetical impacts on ecosystem elements, taking into account existing regional anthropogenic strategies and other expected changes in the regional climate as a consequence of global climate change.

References

Aota, M., Shirasawa, K., Krapivin, V.F., Mkrtchyan, F.A., 1991. In: The System for Data

Processing in Okhotsk Sea Monitoring. Proceedings of the Sixth International Symposium on Okhotsk Sea and Sea Ice, 3-6 February 1991, Mombetsu, Hokkaido, Japan. Okhotsk Sea and Cold Ocean Research Association, Mombetsu, Hokkaido, Japan, pp. 317–318.

Aota, M., Shirasawa, K., Krapivin, V.F., Mkrtchyan, F.A., 1992. In: Simulation Model of the Okhotsk Sea Geoecosystem. Proceedings of the Seventh International Symposium on Okhotsk Sea and Sea Ice, 2–5 February 1992, Mombetsu, Hokkaido, Japan. Okhotsk Sea & Cold Ocean Research Association, Mombetsu, Hokkaido, Japan, pp. 311–313.

Aota, M., Shirasawa, K., Krapivin, V.F., Mkrtchyan, F.A., 2003. In: A Project of the Okhotsk Sea GIMS. Proceedings of the Eigth International Symposium on Okhotsk Sea and Sea Ice, 1–5 February 1993, Mombetsu, Hokkaido, Japan. Okhotsk Sea & Cold Ocean Research Association, Mombetsu, Hokkaido, Japan, pp. 498–500.

Belkin, I.M., Cornillon, P.C., 2004. Surface thermal fronts of the Okhotsk Sea. Pacif. Oceanogr. 2 (1–2), 6–19.

Chattopadhyay, G., Chakraborthy, P., Chattopadhyay, S., 2012. Mann-Kendall trend analysis of tropospheric ozone and its modeling using ARIMA. Theor. Appl. Climatol. 110, 321–328. https://doi.org/10.1007/s00704-012-0617-y.

Dedić, N., Stanier, C., 2017. Towards Differentiating Business Intelligence, Big Data, Data Analytics and Knowledge Discovery. 285 Springer International Publishing, Berlin; Heidelberg (ISSN 1865-1356. OCLC 909580101).

Edvardsen, A., Zhou, M., Tande, K.S., Zhu, Y., 2002. Zooplankton population dynamics: measuring in situ growth and mortality rates using an optical plankton counter. Mar. Ecol. Prog. Ser. 227, 205–219.

Edwards, A.M., Brindley, J., 1999. Zooplankton mortality and the dynamical behaviour of plankton population models. Bull. Math. Biol. 61, 303–339.

Efstathiou, M.N., Varotsos, C.A., 2010. On the altitude dependence of the temperature scaling behaviour at the global troposphere. Int. J. Remote Sens. 31 (2), 343–349.

Efstathiou, M.N., Varotsos, C.A., 2012. Intrinsic properties of Sahel precipitation anomalies and rainfall. Theor. Appl. Climatol. 109 (3–4), 627–633.

Efstathiou, M.N., Varotsos, C.A., 2013. On the 11 year solar cycle signature in global total ozone dynamics. Meteorol. Appl. 20 (1), 72–79.

Heath, M., Werner, F., Chai, F., Megrey, B., Monfray, P., 2004. Challenges of modeling ocean basin ecosystems. Science 304 (5676), 1463–1466.

Herman, A., 2016. Discrete-element bonded-particle sea ice model DESIgn, version 1.3. Model description and implementation. Geosci. Model Dev. 9, 1219–1241.

Ide, K., 2018. In: Situation in the Arctic Region and Japan's Arctic Policy. Proceedings of the 33rd International Symposium on Okhotsk Sea & Polar Oceans 2018, 18–21 February 2018, Mombetsu, Hokkaido, Japan. OSPORA, Mombetsu, Hokkaido, Japan, pp. 1–3.

Ikeda, T., Hirakawa, K., Shiga, N., 2002. Production, metabolism and production/biomass (P/B) ratio of *Metridia pacifica* (Crustacea; Copepoda) in Toyama Bay, southern Japan Sea. Plankton Biol. Ecol. 49 (2), 58–65.

Kaevitser, V.I., Krapivin, V.F., Soldatov, V.Yu., 2013. In: A new Information-Modeling Technology for Monitoring Environment in the Okhotsk Sea. Proceedings of the 28-th International Symposium on Okhotsk Sea & Sea Ice. 17–21 February 2013. Mombetsu, Hokkaido, Japan. The Okhotsk Sea & Cold Ocean Research Association, Mombetsu, Hokkaido, Japan, pp. 295–299.

Kelley, J.J., Krapivin, V.F., 2004. Biocomplexity problem related to the Okhotsk Sea fisheries. In: International Conference DAS, 27–29 June 2004, Suceava, Romania, pp. 52–57.

Kleiber, M., 1932. Body size and metaboliz. Hilgardia 6, 315–332.

Knies, J.L., Kingsolver, J.G., 2010. Erroneous Arrhenius: modified Arrhenius model best explains the temperature dependence of ectotherm fitness. Am. Nat. 176 (2), 227–233.

Krapivin, V.F., 2015. In: The Okhotsk Sea Biocomplexity Model. Proceedings of the 30th International Symposium on Okhotsk Sea & Sea Ice. 15–19 February 2015. Mombetsu, Hokkaido, Japan. The Okhotsk Sea & Cold Ocean Research Association, Mombetsu, Hokkaido, Japan, pp. 223–226.

Krapivin, V.F., Ba Lan, H., 1995. Mathematical model for the dynamics of radionuclides, heavy metals, and petroleum hydrocarbons in the Arctic basin. Phys. Oceanogr. 6 (6), 435–451.

Krapivin, V.F., Mkrtchyan, F.A., 2016. Spectroellipsometric tools for the water quality diagnostics in the Sea of Okhotsk. In: Proceedings of the 31st International Symposium on Okhotsk Sea & Sea Ice, 21–24 February 2016, Mombetsu, Hokaido, Japan. The Okhotsk Sea & Cold Ocean Research Association (OSCORA), Mombetsy, Hokkaido, Japan, pp. 101–104.

Krapivin, V.F., Soldatov, V.Y., 2009. In: Biocomplexity Problem Related to the Okhotsk Sea Ecosystem. Proceedings of the 24th International Symposium on Okhotsk Sea and Sea Ice, 15–20 February 2009, Mombetsu, Hokkaido, Japan. The Okhotsk Sea & Cold Ocean Research Association, Mombetsu, Hokkaido, Japan, pp. 143–146.

Krapivin, V.F., Varotsos, C.A., 2016. Modelling the CO_2 atmosphere-ocean flux in the upwelling zones using radiative transfer tools. J. Atmos. Sol. Terr. Phys. 150, 47–54.

Krapivin, V.F., Cherepenin, V.A., Phillips, G.W., August, R.A., Pautkin, A.Yu., Harper, M.J., Tsang, F.Y., 1998. An application of modeling technology to the study of radionuclear pollutants and heavy metals dynamics in the Angara-Yenisey river system. Ecol. Model. 111 (2–3), 121–134.

Krapivin, V.F., Varotsos, C.A., Soldatov, V.Yu., 2015. New Ecoinformatics Tools in Environmental Science: Applications and Decision-Making. Springer, London, U.K. (903 pp).

Krapivin, V.F., Mkrtchyan, F.A., Soldatov, V.Yu., 2016. In: An Expert System for the Okhotsk Sea investigation. Proceedings of the 31st International Symposium on Okhotsk Sea & Sea Ice, 21–24 February 2016, Mombetsu, Hokaido, Japan. The Okhotsk Sea & Cold Ocean Research Association (OSCORA), Mombetsy, Hokkaido, Japan, pp. 304–307.

Krapivin, V.F., Varotsos, C.A., Nghia, B.Q., 2017a. A modeling system for monitoring

water quality in lagoons. Water Air Soil Pollut. 228 (397), 1–12.

Krapivin, V.F., Varotsos, C.A., Soldatov, V.Yu., 2017b. The Earth's population can reach 14 billion in the 23rd century without significant adverse effects on survivability. Int. J. Environ. Res. Public Health 14 (8), 3–18.

Kwok, R., 2010. Satellite remote sensing of sea-ice thickness and kinematics: a review. J. Glaciol. 56 (200), 1129–1140.

Laurel, B.J., Copeman, L.A., 2018. In: Temperature Impacts on Polar cod (*Boreogadus saida*) During the First Year of Life. Proceedings of the 33-rd International Symposium on Okhotsk Sea & Polar Oceans 2018. 18–21 February 2018, Mombetsu, Hokkaido, Japan. Okhotsk Sea and Polar Oceans Research Association, Mombetsu, Hokkaido, Japan, pp. 4–5.

Legendre, L., Krapivin, V.F., 1992. In: Model for Vertical Structure of Phytoplankton Community in Arctic Regions. Proceedings of the Seventh International Symposium on Okhotsk Sea and Sea Ice, 2–5 February 1992, Mombetsu, Hokkaido, Japan. Okhotsk Sea & Cold Ocean Research Association, Mombetsu, Hokkaido, Japan, pp. 314–316.

Lovejoy, S., Varotsos, C., 2016. Scaling regimes and linear/nonlinear responses of last millennium climate to volcanic and solar forcings. Earth Syst. Dynam. 7 (1), 133–150.

Matoba, S., Shiraiwa, T., Tsushima, A., Sasaki, H., Muravyev, Y.D., 2011. Records of sea-ice extent and air temperature at the Sea of Okhotsk from an ice core of Mount Ichinsky, Kamchatka. Ann. Glaciol. 52 (58), 44–50.

Michener, W.K., Baerwald, T.J., Firth, P., Palmer, M.A., Rosenberger, J.L., Sandlin, E.A., Zimmerman, H., 2001. Defining and unraveling biocomplexity. BioScience 51 (12), 1018–1023.

Mkrtchyan, F.A., Krapivin, V.F., 2011. In: GIMS-Technology in Monitoring Marine Ecosystems. Proceedings of the 26th International Symposium on Okhotsk Sea & Sea Ice. 20–25 February 2011, Mombetsu, Hokkaido, Japan. Okhotsk Sea and Polar Oceans Research Association, Mombetsu, Hokkaido, Japan, pp. 163–166.

Nihashi, S., Ohshima, K.I., Tamura, T., Fukamachi, Y., Saitoh, S., 2009. Thickness and production of sea ice in the Okhotsk Sea coastal polynyas from AMSR-E. J. Geophys. Res. 114 (C10025). https://doi.org/10.1029/2008JC005222.

Ohshima, K.-I., Martin, S., 2004. Introduction to special section: oceanography of the Okhotsk Sea. J. Geophys. Res. 109 (C09S01), 1–3.

Ohshima, K.-I., Nihashi, S., Hashiya, E., Watanabe, T., 2006. Interannual variability of sea ice area in the Sea of Okhotsk: importance of surface heat flux in fall. J. Meteorol. Soc. Jpn. 84 (5), 907–919.

Ohshima, K.-I., Nakanowatari, T., Nakatsuka, T., Nishioka, J., Wakatsuchi, M., 2009. Changes in the Sea of Okhotsk Due to Global Warming – Weakening Pump Function to the North Pacific. PICES Scientific Report No. 36. pp. 16–20.

Pethybridge, H.R., Choy, C.A., Polovina, J.J., Fulton, E.A., 2018. Improving marine ecosystem models with biochemical tracers. Annu. Rev. Mar. Sci. 10, 199–228.

Rohrer, J.P., Jabbar, A., Sterbenz, J.P., 2014. Path diversification for future internet end-to-end resilience and survivability. Telecommun. Syst. 56 (1), 49–67.

Shirasawa, K., Krapivin, V.F., Mkrtchyan, F.A., Kelley, J.J., 2017. In: Biocomplexity problem related to the Okhotsk Sea fisheries. Proceedings of the IX International Symposium "Engineering Ecology – 2017". Moscow, 5–7 December, 2017. The Moscow Sciences Engineering A.S. Popov Society for Radio, Electronics and Communication, Moscow, pp. 75–79.

Takahashi, H., Kasahara, M., Kimata, F., Miura, S., Heki, K., Seno, T., Kato, T., Vasilenko, N., Ivaschenko, A., Bahtiarov, V., Levin, V., Gordeev, E., Korchagin, F., Gerasimenko, M., 1999. Velocity field of around the Sea of Okhotsk and Sea of Japan regions determined from a new continuous GPS network data. Geophys. Res. Lett. 26 (16), 2533–2536.

Tateyama, K., Inoue, J., Hoshino, S., Sasaki, S., Tanaka, Y., 2018. In: Development of a New Algorithm to Estimate Arctic Sea-Ice Thickness Based on Advanced Microwave Scanning Radiometer 2 data. Proceedings of the 33rd International Symposium on Okhotsk Sea & Polar Oceans 2018. 18–21 February 2018. Mombetsu, Hokkaido, Japan. Okhotsk Sea and Polar Oceans Research Association, Mombetsu, Hokkaido, Japan, pp. 47–52.

Varotsos, C., 1987. Quasi-stationary planetary waves and temperature reference atmosphere. Meteorog. Atmos. Phys. 37 (4), 297–299.

Varotsos, C., 2002. The southern hemisphere ozone hole Split in 2002. Environ. Sci. Pollut. Res. 9, 375–376.

Varotsos, C., 2003. What is the lesson from the unprecedented event over Antarctica in 2002. Environ. Sci. Pollut. Res. 10 (2), 80–81.

Varotsos, C., 2004. The extraordinary events of the major, sudden stratospheric warming, the diminutive Antarctic ozone hole, and its split in 2002. Environ. Sci. Pollut. Res. 11 (6), 405–411.

Varotsos, C.A., 2013. The global signature of the ENSO and SST-like fields. Theor. Appl. Climatol. 113 (1–2), 197–204.

Varotsos, C., Cartalis, C., 1991. Re-evaluation of surface ozone over Athens, Greece, for the period 1901–1940. Atmos. Res. 26 (4), 303–310.

Varotsos, C.A., Efstathiou, M.N., 2013. Is there any long-term memory effect in the tropical cyclones? Theor. Appl. Climatol. 114 (3–4), 643–650.

Varotsos, C.A., Efstathiou, M.N., 2019. Has global warming already arrived? J. Atmos. Sol. Terr. Phys. 182, 31–38.

Varotsos, C.A., Krapivin, V.F., 2017. A new big data approach based on geoecological information-modeling system. Big Earth Data 1 (1–2), 47–63.

Varotsos, C.A., Zellner, R., 2010. A new modeling tool for the diffusion of gases in ice or amorphous binary mixture in the polar stratosphere and the upper troposphere. Atmos. Chem. Phys. 10 (6), 3099–3105.

Varotsos, C.A., Franzke, C.L., Efstathiou, M.N., Degermendzhi, A.G., 2014. Evidence for two abrupt warming events of SST in the last century. Theor. Appl. Climatol. 116 (1–2), 51–60.

Varotsos, C.A., Efstathiou, M.N., Christodoulakis, J., 2019. Abrupt changes in global

tropospheric temperature. Atmos. Res. 217, 114–119.

Volkov, A.F., 2018. Present state of the spring plankton community in the northern Okhotsk Sea (1997–2017). In: Izvestia of TINRO. 192. pp. 121–135 (in Russian).

Xue, Y., He, X.W., Xu, H., Guang, J., Guo, J.P., Mei, L.L., 2014. China collection 2.0: the aerosol optical depth dataset from the synergetic retrieval of aerosol properties algorithm. Atmos. Environ. 95, 45–58. https://doi.org/10.1016/j.atmosenv.2014.06.019.

Zakharkov, S.P., Vladimirov, A.S., Shtraikhert, E.A., Shi, X., Gladkich, R.V., Buzoleva, L.S., 2017. Production characteristics of bacteria and phytoplankton in the Sea of Okhotsk and Bering Sea during spring-summer. Microbiology 86 (3), 387–394.

Zhabin, I.A., Abrosimova, A.A., Dubina, V., Nekrasov, D.A., 2010. Influence of the Amur River runoff on the hydrological conditions of the Amur Liman and Sakhalin Bay (Sea of Okhotsk) during the spring-summer flood. Russ. Meteorol. Hydrol. 35 (4), 295–300.